# Bulk Heterojuction Solar Cells Containing 6,6-Dicyanofulvenes as n-Type Additives

**Trisha L. Andrew and Vladimir Bulović***

Department of Electrical Engineering and Computer Science, Massachusetts Institute of Technology, 77 Massachusetts Avenue, Cambridge, Massachusetts 02139, United States

**ABSTRACT**

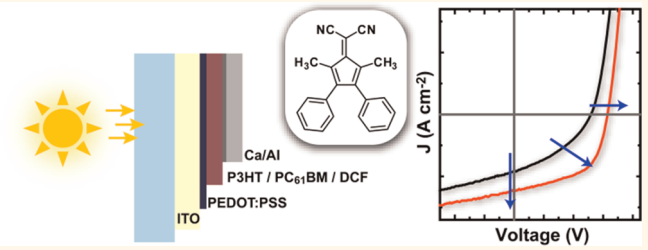


**P3HT/$PC_{61}BM$ bulk heterojunction solar cells containing varying amounts of different 6,6-dicyanofulvenes (DCFs) were fabricated and characterized. Photovoltaic cells containing ternary mixtures of P3HT, 0.5 equiv of $PC_{61}BM$, and 0.5 equiv of 1,4-dimethyl-2,3-diphenyl-DCF (by weight) displayed average power conversion efficiencies of up to 4.5% under AM 1.5 irradiation, compared to 2.9% for reference P3HT—$PC_{61}BM$ solar cells. It was found that 1,4-dimethyl-2,3-diphenyl-6,6-dicyanofulvene could replace up to 50 wt % of $PC_{61}BM$ in 1:1 P3HT—$PC_{61}BM$ solar cells without sacrificing device performance.**

**KEYWORDS:** photovoltaic · polythiophene · fullerene · additive · fulvene · substitute

Donor—acceptor bulk heterojunction (BHJ) solar cells formed by mixtures of regioregular poly(3-hexylthiophene) (P3HT) and soluble fullerene derivatives, such as $PC_{61}BM$ and $PC_{71}BM$, are a benchmark organic photovoltaic (OPV) structure, with average power conversion efficiencies (PCEs) of about 5% under AM 1.5 conditions (100 mW/cm$^2$).[1] In this study, we show that a similar performance can be obtained with 6,6-dicyanofulvenes (DCFs) as additives or fullerene substitutes in P3HT/$PC_{61}BM$ OPVs.

A variety of device and material factors limit the performance of BHJ solar cells, but the properties of the photoactive layer are the primary determinant of the maximum achieveable PCE.[2] The ideal donor—acceptor mixture in a BHJ structure should exhibit a bicontinuous network with domain widths within twice that of the exciton diffusion length and a high donor—acceptor interfacial area to favor exciton dissociation and efficient transport of separated charges to the respective electrodes.[3] Over the past few years, optimization of the donor component of BHJ solar cells[4−13] has resulted in polymer—fullerene devices with PCEs close to 8%.[14,15] These advances were attributed to a combination of improved energy band lineup between the donor polymer and fullerene acceptors and increased near-infrared (NIR) absorption.[4−15] Additionally, the use of additives, including high boiling point alkyl dihalides that act as cosolvents[16] and main-chain block copolymers,[17−19] to improve the performance of P3HT—$PC_{61}BM$ solar cells has been reported in the past. In both of these cases, small amounts of additives lead to increases in short circuit current ($J_{SC}$) values due to favorable morphological effects; however, the presence of greater than approximately 10 wt % of these additives proved detrimental to the PCE of the resulting solar cells.[16−19]

Thus far, comparable effort has not been expended on optimizing the acceptor component of BHJ solar cells, and soluble fullerene derivatives, such as $PC_nBM$ ($n$ = 61, 71), are largely accepted as the default electron-transporting materials in the BHJ OPVs.[2−15,20] Indeed, fullerene-based acceptors have a number of advantages, such as high electron mobilities, photochemical and electrochemical stability, and energy bands that are compatible with many potential donor materials (including both molecular and polymeric donors).[2,4−15,20] Disadvantages in the use of $PC_nBM$ as the acceptor in BHJs include low light absorption, charge transport that is sensitive to film morphology,[21,22] high rates of charge recombination across the donor—acceptor interface,[23] and significant energy losses during forward electron transfer from many donor materials.[2]

* Address correspondence to bulovic@mit.edu.

Received for review October 21, 2011 and accepted May 30, 2012.

**Published online May 30, 2012**
10.1021/nn301851k

© 2012 American Chemical Society

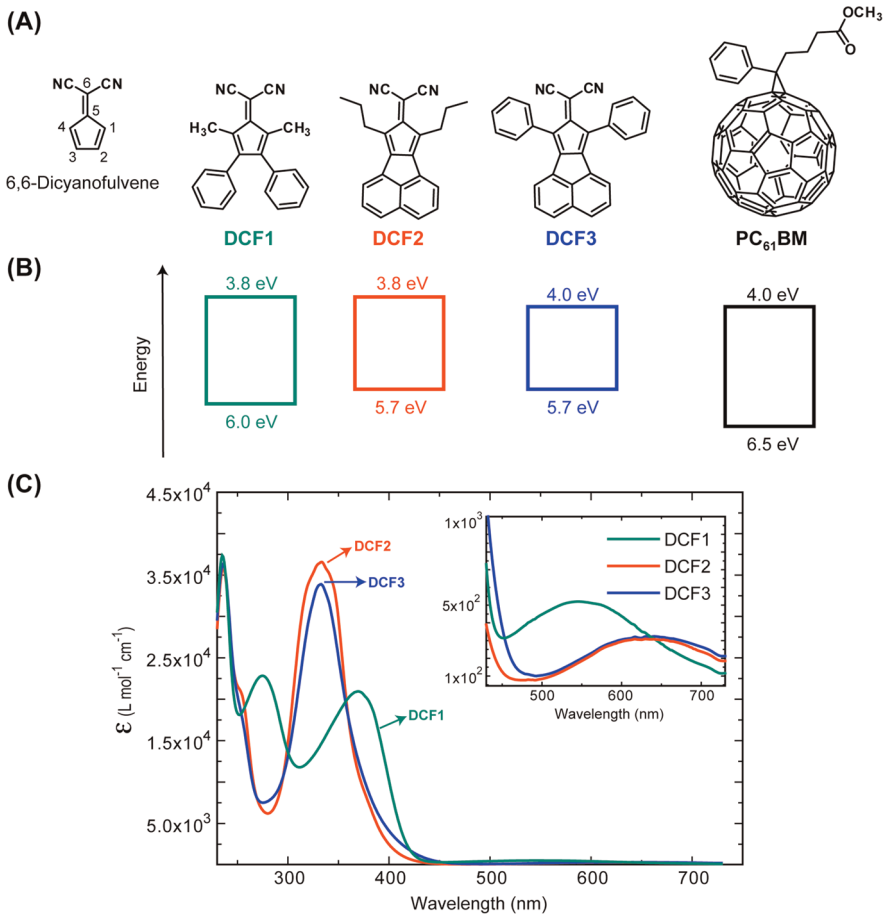


**Figure 1. (A) Structures of the 6,6-dicyanofulvenes (DCFs) used in this study. (B) HOMO and LUMO values of DCF1−3 and $PC_{61}BM$. (C) Absorption spectra of DCF1−3 in $CHCl_3$. The absorption spectra of 50 nm thick films of DCF1−3 are observed to be similar to their respective solution absorption spectra. The DCFs do not display observable luminescence at room temperature.**

Moreover, the relatively limited availability and high cost of fullerenes is a nontrivial issue and has, thus far, proved a bottleneck in the development of fullerene science in engineering and pharmaceuticals.[24]

Select alternative electron transporters have been investigated as $PC_nBM$ substitutes in OPVs, including (non-exhaustively) endohedral fullerenes;[25] CdSe nanocrystals;[26−28] $TiO_2$ nanoparticles;[29] various monomeric, oligomeric, and polymeric 3,4,9,10-perylenetetracarboxydiimides (PTCDIs)[30−33] and 1,4,5,8-naphthalenetetracarboxydiimides (NTCDIs);[34] a benzimidazobenzophenanthroline ladder polymer (BBL);[35] poly(*p*-phenylene cyanovinylene)s (CNPPVs);[36,37] carbon nanotubes;[38−44] thiophene-1,1-dioxide derivatives;[45] and vinazene-type small molecule acceptors.[46−48] Although endohedral fullerenes are superior acceptor materials compared to $PC_nBM$, they are difficult to produce and purify in large quantities. Relatively high PCEs were obtained with P3HT−CdSe nanocrystal BHJs; however, the primary limitation of nanocrystal-based acceptors is their inability to form low-resistance charge percolation networks when mixed with P3HT.[26−28,49,50] In the case of P3HT−$TiO_2$ mixtures, a significant drawback is the approximately 1 eV of energy loss when electrons transfer from the polymer to the $TiO_2$.[2] In the case of small molecule PTCDI acceptors, relatively high PCEs (>2% under AM 1.5 conditions, 100 mW/cm$^2$) were only obtained with small molecule donors, such as copper phthalocyanine (CuPc)[3] since polymer−PTCDI mixtures undergo detrimental macroscopic phase separation.[51] In the case of BBL, only bilayer devices were accessible due to the limited solubility of BBL, and such devices (with a poly(*p*-phenylene vinylene) donor) exhibited a PCE of approximately 1%.[35] Similarly, solar cells fabricated with either CNPPVs, polymeric PTCDIs, or solution-processable small molecule acceptors, such as vinazene-type compounds and thiophene-1,1-dioxide derivatives, yielded PCEs of only up to 1%. Notably, the use of such non-fullerene acceptors in BHJs generally resulted in much larger open circuit voltages ($V_{OC}$), with average values of approximately 1.0 V (as compared to a $V_{OC}$ of 0.6 V for P3HT/$PC_{61}BM$ BHJ OPVs).[30−37,45−50]

Previously, DCFs were reported as electron-transporting materials that displayed comparable electron affinities (EAs) and electrochemical stabilities to

$PC_{61}BM$ and were easily accessible *via* straightforward, low-cost synthetic protocols.[52] In this contribution, we investigate the use of DCFs as additives and/or fullerene substitutes in P3HT/$PC_{61}BM$ solar cells.

## RESULTS AND DISCUSSION

Three different DCFs are synthesized, **DCF1**, **DCF2**, and **DCF3** (Figure 1A), that differ in their solid-state packing structure due to varying molecular volume and steric bulk around the 6,6-dicyanofulvene core.[52] The HOMO and LUMO values of **DCF1**−**3** (as obtained through cyclic voltammetry; see Methods section) are shown in Figure 1B. We note that the electron affinities of **DCF1**−**3** are comparable to that of $PC_{61}BM$. The absorption spectra of **DCF1**−**3** (Figure 1C) are dominated by strong $\pi-\pi^*$ transitions at wavelengths less than 400 nm. Additionally, **DCF1**−**3** display weak absorbance bands in the visible region.

Steady-state fluorescence quenching studies of P3HT with **DCF1**−**3** in chloroform solutions reveal that **DCF1**−**3** quench the excited state of P3HT (see Supporting Information), thus confirming that these dicyanofulvenes are capable of promoting exciton dissociation in solar cells containing P3HT. The steady-state Stern−Volmer quenching constant ($K_{SV}$) of **DCF1** is calculated to be $2.3 \times 10^3\ M^{-1}$, which is similar to that obtained for $PC_{61}BM$ (see Supporting Information). **DCF2** and **DCF3** display lower $K_{SV}$ values of $2.0 \times 10^3$ and $1.7 \times 10^3\ M^{-1}$, respectively, indicating weaker interactions with the excited state of P3HT compared to **DCF1** and $PC_{61}BM$.

Electron transport through **DCF1**−**3** is investigated in both top-gated field-effect transistors (FETs) and electron-only space-charge-limited current (SCLC) devices. FETs fabricated using thermally evaporated films of **DCF1**−**3** and CVD-deposited parylene-C as the top-gate dielectric display n-channel conduction and negligible p-channel conduction (see Supporting Information). The extracted saturation regime electron mobilities for **DCF1**, **DCF2**, and **DCF3** are $1.1 \times 10^{-3}$, $2.2 \times 10^{-3}$, and $1.4 \times 10^{-4}\ cm^2\ V^{-1}\ s^{-1}$, respectively (in our hands, a PCBM top-gated FET fabricated under similar conditions afforded $\mu_e = 8.1 \times 10^{-3}\ cm^2\ V^{-1}\ s^{-1}$). However, the SCLC electron mobilities of **DCF1**−**3** were observed to be at least an order of magnitude lower than those obtained in the lateral FET device architectures (see Supporting Information), thus suggesting that electron transport is highly anisotropic in thermally evaporated amorphous films of **DCF1**−**3**.

The performance of **DCF1**−**3** as acceptor components in P3HT-based solar cells is first investigated in layered device architectures. The *J*−*V* characteristics under 1 sun illumination of devices containing a 40 nm thick P3HT donor layer and various acceptor layers are shown in Figure 2B. The use of **DCF1** and **DCF2** affords photodiode behavior similar to that observed with $C_{60}$. Solar cells with **DCF1** display PCEs similar to that of $C_{60}$

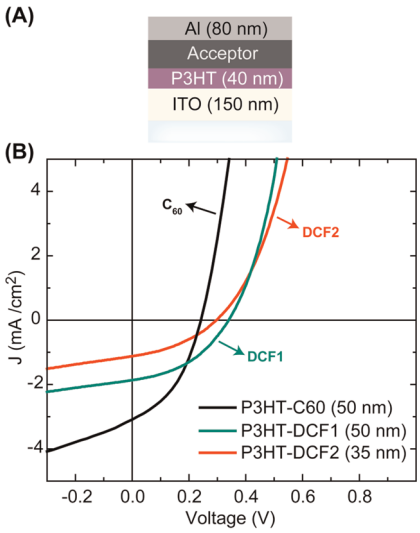


(C)

| Acceptor | $V_{OC}$ (V) | $J_{SC}$ (mA cm$^{-2}$) | FF | PCE (%) |
|---|---|---|---|---|
| C60 | 0.24 | 3.1 | 0.40 | 0.30 |
| DCF1 | 0.33 | 1.9 | 0.41 | 0.26 |
| DCF2 | 0.30 | 1.2 | 0.33 | 0.12 |

**Figure 2. (A) Cross section of a layered device structure containing a P3HT donor layer and various acceptor layers. (B) *J*−*V* characteristics under AM 1.5 illumination (100 mW/cm$^2$) of the solar cells shown in (A). Each plotted curve represents an average of the *J*−*V* curves of eight different devices. The optimized acceptor layer thicknesses are as follows: 50 nm $C_{60}$; 50 nm DCF1; and 35 nm DCF2. (C) Tabular summary of pertinent metrics for the same devices as in (B).**

devices but have higher open circuit voltages ($V_{OC}$) and lower $J_{SC}$. Using acenaphthene-derived **DCF2** as the acceptor produces a lower $V_{OC}$ and $J_{SC}$ than with **DCF1**. Moreover, devices with **DCF3** as an acceptor yield significantly low overall current densities ($J_{SC}$ = 0.078 mA/cm$^2$), and therefore, the *J*−*V* characteristics of these devices are not plotted in Figure 2B.

Bulk heterojunction photovoltaic cells containing ternary mixtures of P3HT/$PC_{61}BM$/**DCF1**-**3** in the active layer are investigated to identify (a) whether the presence of DCF additives can improve the PCE of P3HT−$PC_{61}BM$ solar cells and (b) whether the nature of the substituents around the 6,6-dicyanofulvene core influence observable device metrics. Our standard device architecture is as follows: ITO/PEDOT:PSS (40 nm)/active layer/Ca (25 nm)/Al (80 nm). We initially investigate BHJ devices with 75 nm thick photoactive layers. The *J*−*V* curves for ternary mixtures containing **DCF1**−**3** (1:1 P3HT/$PC_{61}BM$ by weight + 0.5 weight equivalent **DCF1**/**2**/**3**) are shown in Figure 3A. Considering the high additive loading employed, the bulky **DCF3** (which displays the highest steric bulk around the 6,6-dicyanofulvene core) proved significantly detrimental to the performance of a BHJ P3HT−$PC_{61}BM$ solar cell. This is consistent with the poor performance observed for layered devices fabricated with **DCF3** as the acceptor component. In contrast, adding **DCF1** and **DCF2** increased the $J_{SC}$ and fill factor (FF) and slightly

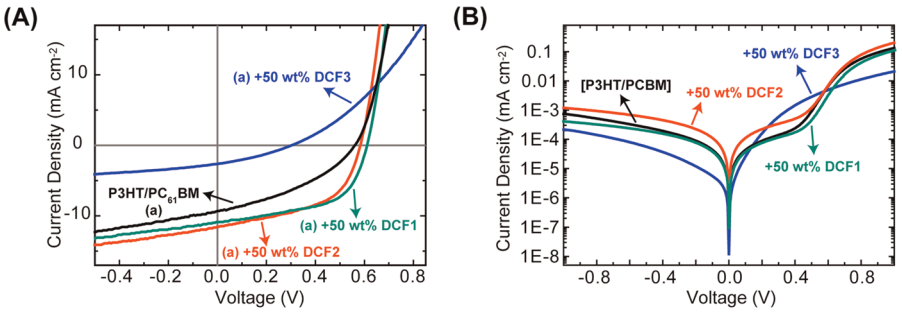


(C)

| | $V_{OC}$ (V) | $J_{SC}$ (mA cm$^{-2}$) | FF | PCE (%) |
|---|---|---|---|---|
| 1:1 P3HT/$PC_{61}BM$ | 0.56 | 9.5 | 0.53 | 2.8 |
| + 50 wt% **DCF1** | 0.61 | 11.1 | 0.55 | 3.7 |
| + 50 wt% **DCF2** | 0.58 | 11.8 | 0.54 | 3.7 |
| + 50 wt% **DCF3** | 0.30 | 2.7 | 0.30 | 0.2 |

**Figure 3. (A) *J*−*V* characteristics of bulk heterojunction photovoltaic cells fabricated with ternary mixtures containing DCF1−3 (1:1 P3HT/$PC_{61}BM$ + 50 wt % DCF) and illuminated under AM 1.5 conditions (100 mW/cm$^2$). The active layer thickness is 75 ± 5 nm. (B) Dark current *J*−*V* curves for the same devices as in (A). The *J*−*V* characteristics (light and dark) for a reference 1:1 P3HT−$PC_{61}BM$ solar cell fabricated under similar conditions is provided. (C) Tabular summary of pertinent metrics for the same devices as in (A).**

increased the $V_{OC}$ of 1:1 P3HT−$PC_{61}BM$ solar cells. It is also notable that a high loading (50 wt %) of **DCF1** and **DCF2** did not increase the series resistance of the devices, as evidenced by the absence of change in the slope of forward-biased PVs under illumination. Devices containing 50 wt % added **DCF1** or **DCF2** displayed an average PCE of 3.6% (measured over five devices each), whereas reference 1:1 P3HT−$PC_{61}BM$ solar cells fabricated under similar conditions displayed average PCEs of 2.9%. From the averaged dark current *J*−*V* curves (Figure 3B), it is evident that PVs containing **DCF1** yield the lowest dark currents. We, therefore, chose to optimize the weight ratio of this additive in P3HT−$PC_{61}BM$ devices.

Pertinent metrics from a series of devices containing P3HT−$PC_{61}BM$−**DCF1** ternary mixtures are plotted in Figure 4 (for each measurement, the average values for five identical devices are indicated with the error bars accounting for data spread). As many combinations of weight ratios can be envisioned for ternary systems, we narrowed our study to two regimes: excess total acceptor ($PC_{61}BM$ + **DCF1**) concentration relative to P3HT and 1:1 P3HT−total acceptor ratio. In the former case, the concentration of P3HT in the resulting active layer is systematically reduced with increasing **DCF1** content, whereas in the latter case, the P3HT concentration remains static while only the ratios of $PC_{61}BM$ and **DCF1** are varied. We also compare all devices containing **DCF1** to both reference 1:1 P3HT−$PC_{61}BM$ cells and solar cells containing 1:2 P3HT−$PC_{61}BM$. In the case where excess total acceptor is employed, the $V_{OC}$ and $J_{SC}$ are found to steadily increase with **DCF1** concentration until approximately 50 wt %, beyond which the device performance is negatively affected by the high DCF loading. Notably, even though the fraction of P3HT—the primary absorbing component—is

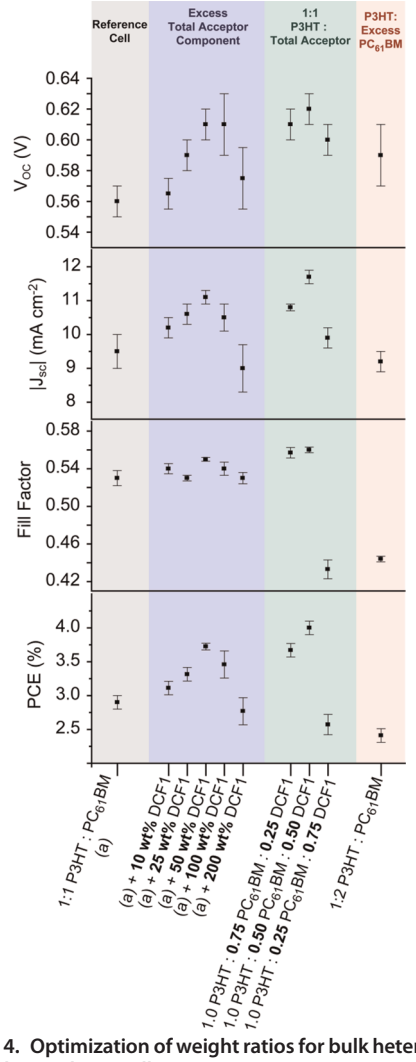


**Figure 4. Optimization of weight ratios for bulk heterojunction photovoltaic cells containing ternary mixtures of P3HT−$PC_{61}BM$−DCF1. The thickness of the active layer for all devices is 75 ± 5 nm. Shown are $V_{OC}$, $J_{SC}$, FF, and PCE for various combinations of the three component materials.**

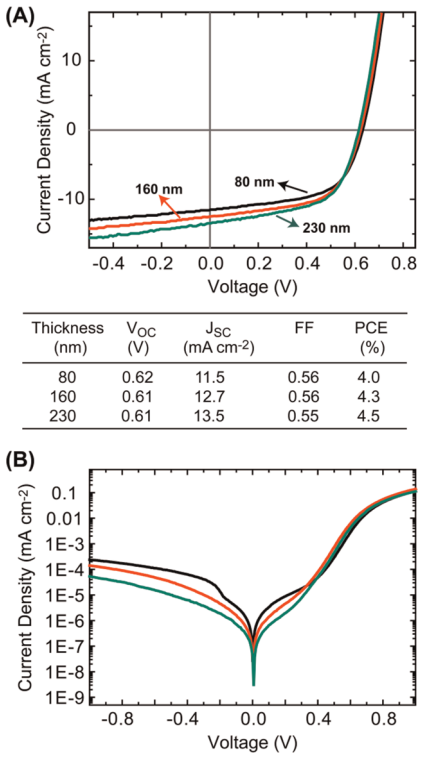


| Thickness (nm) | $V_{OC}$ (V) | $J_{SC}$ (mA cm$^{-2}$) | FF | PCE (%) |
|---|---|---|---|---|
| 80 | 0.62 | 11.5 | 0.56 | 4.0 |
| 160 | 0.61 | 12.7 | 0.56 | 4.3 |
| 230 | 0.61 | 13.5 | 0.55 | 4.5 |

**Figure 5. (A) *J*–*V* characteristics of P3HT + 0.5 $PC_{61}BM$ + 0.5 DCF1 bulk heterojunction solar cells of different active layer thickness under AM 1.5 illumination (100 mW/cm$^2$). (B) Dark current *J*–*V* curves for the same devices. Each plotted curve represents an average of the *J*–*V* curves of five different devices.**

decreasing, the observed PCE increases with added **DCF1**. External quantum efficiency measurements for these devices reflect the same trend (see Supporting Information), thus suggesting that the DCF additives improve charge transport and/or charge collection in P3HT–$PC_{61}BM$ solar cells.

If the ratios of $PC_{61}BM$ and **DCF1** are varied while keeping the concentration of P3HT static, high $V_{OC}$ and $J_{SC}$ values are obtained if **DCF1** is used to replace $PC_{61}BM$, up to a 50% concentration by weight. For instance, PCEs of up to 4.1% are obtained with ternary mixtures composed of 1.0 P3HT + 0.5 $PC_{61}BM$ + 0.5 **DCF1**. However, **DCF1** does not perform well as a majority acceptor (possibly due to poor charge transport properties of the resulting blend), and solar cells containing 1.0 P3HT + 0.25 $PC_{61}BM$ + 0.75 **DCF1** perform slightly worse than reference 1:1 P3HT–$PC_{61}BM$ cells. Moreover, photovoltaic devices fabricated with P3HT–**DCF1** mixtures (excluding $PC_{61}BM$) display negligible rectification and PCEs (see Supporting Information).

Lastly, the thickness of the active layer in cells containing 1.0 P3HT + 0.5 $PC_{61}BM$ + 0.5 **DCF1** was varied (Figure 5). As expected, average $J_{SC}$ values (over eight devices) increased with increasing layer thickness, while only slight variations in $V_{OC}$ is observed. Devices fabricated with 230 nm active layers displayed PCEs of up to 4.5%. This value is close to the 5% PCE reported for optimized P3HT–$PC_{61}BM$ solar cells,[1] although we halved the amount of $PC_{61}BM$ used and did not require the use of alkyl dihalide additives and extensive optimization of the processing solvent and annealing time/temperature.

X-ray diffractograms (XRDs) of various ternary mixtures of P3HT–$PC_{61}BM$–**DCF1** displayed the signature order peaks of P3HT lamellae (see Supporting Information), indicating that the high loadings of **DCF1** used in this study did not disrupt the crystallinity and, therefore, the transport properties of P3HT–$PC_{61}BM$ blends. However, XRDs of binary P3HT/**DCF1** mixtures did not display any order peaks and were observed to be amorphous, thus possibly providing an explanation for the poor performance of the corresponding solar cells.

## CONCLUSION

In conclusion, up to 4.5% power conversion efficiencies were obtained in photovoltaic cells containing ternary mixtures of P3HT, $PC_{61}BM$, and a 6,6-dicyanofulvene (DCF) in the active layer, compared to 2.9% for reference P3HT–$PC_{61}BM$ solar cells. It was found that 1,4-dimethyl-2,3-diphenyl-6,6-dicyanofulvene could replace up to 50 wt % of $PC_{61}BM$ in 1:1 P3HT–$PC_{61}BM$ solar cells without sacrificing device performance. The substituents at the 1,4-positions of the 6,6-dicyanofulvene core were found to influence the efficacy of the DCF additives, and the presence of bulky phenyl moieties proved detrimental to additive performance. Moreover, the use of alkyl dihalide additives and extensive optimization were not necessary to achieve substantially improved device performance (relative to P3HT–$PC_{61}BM$ devices) with the DCF additive. Although DCFs do not yield practically functional photovoltaic devices when used in binary mixtures with P3HT, our preliminary studies suggest that DCFs are promising n-type additives that increase the short circuit current and fill factor of polymer-based OPVs.

## METHODS

**Materials.** Electronic-grade regioregular P3HT ($M_n$ 30 000–60 000) and $PC_{61}BM$ were purchased from Aldrich and used without further purification. **DCF1**–**3** were synthesized as previously reported.[52] LUMO and HOMO values were calculated from the cyclic voltammograms of **DCF1**–**3** (provided in ref 52) and the optical band gap of the respective compounds.

**Device Fabrication.** Patterned indium tin oxide (ITO)-coated glass substrates were sonicated in acetone (30 min) and isopropyl

alcohol (30 min) and oxygen plasma-cleaned (3 min) immediately prior to deposition of the PEDOT:PSS layer. PEDOT:PSS (2−5 wt % in water, Aldrich) was spin-coated in a nitrogen atmosphere at 4000 rpm and annealed at 150 °C (using a hot plate) for 15 min under nitrogen. A 40 nm PEDOT layer was thus obtained. For the active layer, a 10 mg/mL solution of 1:1 total polymer/$PC_{61}BM$ in 1,2-dichlorobenzene (DCB) was employed (in a representative example, 2.9 mg of P3HT, 1.5 mg of **DCF1**, and 3.1 mg of $PC_{61}BM$ were dissolved in 0.3 mL of DCB). A 60 $\mu$L aliquot of this solution was then spin-coated onto the PEDOT layer at 1000 rpm under nitrogen. The substrate was taken from the spin chuck and immediately placed under an inverted Petri dish inside the glovebox for 10 min to encourage solvent annealing from the small amount of residual DCB on the substrate. Next, the solar cells were placed on a 150 °C hot plate and annealed for 45 min under nitrogen. A 75−80 nm thick active layer was thus obtained. In order to obtain thicker active layers, a 20 mg/mL (160 nm thick film) or a 30 mg/mL (230 nm thick film) solution of the ternary mixture was used. Following this deposition procedure, the top electrode was deposited by evaporation of a 25 nm thick film of Ca followed by 80 nm thick film of Al. Each device has an area of 1.2 $mm^2$.

For the layered solar cells, 40 nm thick PEDOT:PSS on ITO was fabricated as described above. A 40 nm thick layer of P3HT was then spin-cast from a 10 mg/mL solution of P3HT in DCB at 1000 rpm and annealed at 150 °C for 40 min under nitrogen. The acceptor layer was then deposited by thermal evaporation under ultrahigh vacuum ($10^{-6}$ Torr), followed by an aluminum electrode (80 nm) through an aligned shadow mask. The thicknesses of the acceptor layers were as follows: 50 nm $C_{60}$, 50 nm **DCF1**, 35 nm **DCF2**.

For the top-gated FETs, gold interdigitated electrode arrays (with length and width of $L$ = 10 $\mu$m and $W$ = 12 mm, respectively) were fabricated on substrates of D263 borosilicate glass by e-beam evaporation of 2.5 nm thick film of Ti followed by 45 nm thick film of Au and then patterned with liftoff. Following solvent cleaning, substrates were subjected to oxygen plasma for 30 s and submerged overnight in a 0.1 M solution of (2-phenylethyl)trichlorosilane in toluene. After 1 min of sonication in isopropyl alcohol, substrates were dried with nitrogen and transferred into a nitrogen environment. Fifty nanometer thick films of **DCF1**−**3** were deposited by thermal evaporation at ultrahigh vacuum ($10^{-6}$ Torr). Films of parylene-C were then deposited using diX-C dimer from Daisan Kasei in a homemade CVD reactor. The deposition pressure of the vacuum system was approximately $10^{-3}$ Torr, and the measured parylene-C thickness was 478 nm. An aluminum gate electrode was then deposited by thermal evaporation through an aligned shadow mask.

For the electron-only space-charge-limited current (SCLC) devices, 40 nm thick PEDOT:PSS on ITO was prepared as described above. Films of **DCF1** (250 nm), **DCF2** (200 nm), and **DCF3** (90 nm) were thermally evaporated under ultrahigh vacuum ($10^{-6}$ Torr), followed by an aluminum electrode (80 nm) through an aligned shadow mask. Note that the >500 meV barrier to hole injection at the PEDOT:PSS interface renders hole injection negligible and ensures unipolar electron conduction under forward bias.[53]

**Characterization.** The current−voltage characteristics of the devices were measured using a Keithley 6487 sourcemeter. The devices were illuminated through the glass substrate using an Oriel 96000 150 W full spectrum solar simulator. Spectral mismatch was not corrected in these measurements. For measurement of external quantum efficiencies, the broad-band light from a 1000 W Xe lamp was optically chopped and focused into an Acton Spectrapro 300i monochromator. A calibrated silicon photodetector was used to measure the optical power of the output, which was subsequently focused onto the device under study. A lock-in amplifier provided with the reference signal from the optical chopper (45 Hz) was used to extract a measurement of the AC photocurrent. For the FETs, an Agilent 4156C semiconductor parameter analyzer was used to acquire transfer and output characteristics.

**XRD.** X-ray diffraction was measured using Cu K$\alpha$ radiation on an Inel CPS 120 position-sensitive detector with a XRG 2000 generator and a fine-focus X-ray tube. The detector was calibrated using mica and silicon standards which were obtained from the National Bureau of Standards (NBS).

*Conflict of Interest:* The authors declare no competing financial interest.

*Acknowledgment.* We thank T. M. Swager for providing access to synthetic facilities and graciously donating reagents and starting materials. This work was supported by Eni S.p.A under the Eni-MIT Solar Frontiers Program.

*Supporting Information Available:* Quenching studies, external quantum efficiencies, FETs, XRD data, and solar cells fabricated with select binary mixtures. This material is available free of charge *via* the Internet at http://pubs.acs.org.

## REFERENCES AND NOTES

1. Brabec, C. J.; Gowrisanker, S.; Halls, J. J. M.; Laird, D.; Jia, S.; Williams, S. P. Polymer−Fullerene Bulk-Heterojunction Solar Cells. *Adv. Mater.* **2010**, *22*, 3839–3856 and references therein.
2. Coakley, K. M.; McGehee, M. D. Conjugated Polymer Photovoltaic Cells. *Chem. Mater.* **2004**, *16*, 4533–4542.
3. Forrest, S. R. The Limits to Organic Photovoltaic Cell Efficiency. *MRS Bull.* **2005**, *30*, 28–32.
4. Roncali, J. Molecular Bulk Heterjunctions: An Emerging Appraoch to Organic Solar Cells. *Acc. Chem. Res.* **2009**, *42*, 1719–1730.
5. Wong, W.-Y.; Ho, C.-L. Organometallic Photovoltaics: A New and Versatile Approach for Harvesting Solar Energy Using Conjugated Polymetallaynes. *Acc. Chem. Res.* **2010**, *43*, 1246–1256.
6. Blouin, N.; Leclerc, M. Poly(2,7-carbazoles)s: Structure−Property Relationships. *Acc. Chem. Res.* **2008**, *41*, 1110–1119.
7. Beaujuge, P. M.; Amb, C. M.; Reynolds, J. R. Spectral Engineering in $\pi$-Conjugated Polymers with Intramolecular Donor−Acceptor Interactions. *Acc. Chem. Res.* **2010**, *43*, 1396–1407.
8. Chen, J.; Cao, Y. Development of Novel Conjugated Donor Polymers for High Efficiency Bulk-Heterojunction Photovoltaic Devices. *Acc. Chem. Res.* **2009**, *42*, 1709–1718.
9. Nguyen, L. H.; Hoppe, H.; Erb, T.; Günes, S.; Gobsch, G.; Sariciftci, N. S. Effecs of Annealing on the Nanomorphology and Performance of Poly(alkylthiophene):Fullerene Bulk-Heterojunction Solar Cells. *Adv. Funct. Mater.* **2007**, *17*, 1071–1078.
10. Wu, P.-T.; Ren, G.; Jenekhe, S. A. Crystalline Random Conjugated Copolymers with Multiple Side Chains: Tunable Intermolecular Interactions and Enhanced Charge Transport and Photovoltaic Properties. *Macromolecules* **2010**, *43*, 3306–3313.
11. Ohshimizu, K.; Takahashi, A.; Rho, Y.; Higashihara, T.; Ree, M.; Ueda, M. Synthesis and Characterization of Polythiophenes Bearing Aromatic Groups at the 3-Position. *Macromolecules* **2011**, *44*, 719–727.
12. Gendron, D.; LeClerc, M. New Conjugated Polymers for Plastic Solar Cells. *Energy Environ. Sci.* **2011**, *4*, 1225–1237.
13. Cheng, Y.-J.; Yang, S.-H.; Hsu, C.-S. Synthesis of Conjugated Polymers for Organic Solar Cell Applications. *Chem. Rev.* **2009**, *109*, 5868–5923.
14. Chen, H.-Y.; Hou, J.; Zhang, S.; Liang, Y.; Yang, G.; Yang, Y.; Yu, L.; Wu, Y.; Li, G. Polymer Solar Cells with Enhanced Open-Circuit Voltage and Efficiency. *Nat. Photonics* **2009**, *3*, 649–653.
15. Liang, Y.; Yu, L. A New Class of Semiconducting Polymers for Bulk Heterojunction Solar Cells with Exceptionally High Performance. *Acc. Chem. Res.* **2010**, *43*, 1227–1236.
16. Lee, J. K.; Ma, W. L.; Brabec, C. J.; Yuen, J.; Moon, J. S.; Kim, J. Y.; Lee, K.; Bazan, G. C.; Heeger, A. J. Processing Additives for Improved Efficiency from Bulk Heterojunction Solar Cells. *J. Am. Chem. Soc.* **2008**, *130*, 3619–3623.
17. Tsai, J.-H.; Lai, Y.-C.; Higashihara, T.; Lin, C.-J.; Ueda, M.; Chen, W.-C. Enhancement of P3HT/PCBM Photovoltaic

Efficiency Using the Surfactant of Triblock Copolymer Containing Poly(3-hexylthiophene) and Poly(4-vinyltriphenylamine) Segments. *Macromolecules* **2010**, *43*, 6085–6091.
18. Sivula, K.; Ball, Z. T; Watanabe, N.; Fréchet, J. M. Amphiphilic Diblock Copolymer Compatibilizers and Their Effect on the Morphology and Performance of Polythiophene:Fullerene Solar Cells. *Adv. Mater.* **2006**, *18*, 206–210.
19. Yang, C.; Lee, J. K.; Heeger, A. J.; Wudl, F. Well-Defined Donor–Acceptor Rod-Coil Diblock Copolymers Based on P3HT Containing $C_{60}$: The Morphology and Role as a Surfactant in Bulk-Heterojunction Solar Cells. *J. Mater. Chem.* **2009**, *19*, 5416–5423.
20. Hains, A. W.; Liang, Z.; Woodhouse, M. A.; Gregg, B. A. Molecular Semiconductors in Organic Photovoltaic Cells. *Chem. Rev.* **2010**, *110*, 6689–6735.
21. Groves, C.; Reid, O. G.; Ginger, D. S. Heterogeneity in Polymer Solar Cells: Local Morphology and Performance in Organic Photovoltaics Studied with Scanning Probe Microscopy. *Acc. Chem. Res.* **2010**, *43*, 612–620.
22. Verploegen, E.; Mondal, R.; Bettinger, C. J.; Sok, S.; Toney, M. F.; Bao, Z. Effects of Thermal Annealing Upon the Morphology of Polymer–Fullerene Blends. *Adv. Funct. Mater.* **2010**, *20*, 3519–3529.
23. Clarke, T. M.; Durrant, J. R. Charge Photogeneration in Organic Solar Cells. *Chem. Rev.* **2010**, *110*, 6736–6767.
24. Wudl, F. Fullerene Materials. *J. Mater. Chem.* **2002**, *12*, 1959–1963.
25. Ross, R. B.; Cardona, C. M.; Guldi, D. M.; Sankaranarayanan, S. G.; Reese, M. O.; Kopidakis, N.; Peet, J.; Walker, B.; Bazan, G. C.; Keuren, E. V.; *et al.* Endohedral Fullerenes for Organic Photovoltaic Devices. *Nat. Mater.* **2009**, *8*, 208–212.
26. Huynh, W. U.; Dittmer, J. J.; Alivisatos, A. P. Hybrid Nanorod–Polymer Solar Cells. *Science* **2002**, *295*, 2425–2427.
27. Kamat, P. V. Quantum Dot Solar Cells. Semiconductor Nanocrystals as Light Harvesters. *J. Phys. Chem. C* **2008**, *112*, 18737–18753.
28. Dayal, S.; Kopidakis, N.; Olson, D. C.; Ginley, D. S.; Rumbles, G. Photovoltaic Devices with a Low Band Gap Polymer and CdSe Nanostructures Exceeding 3% Efficiency. *Nano Lett.* **2010**, *10*, 239–242.
29. Arango, A. C.; Carter, S. A.; Brock, P. J. Charge Transfer in Photovoltaics Consisting of Interpenetrating Networks of Conjugated Polymer and $TiO_2$ Nanoparticles. *Appl. Phys. Lett.* **1999**, *74*, 1698–1701.
30. Karak, S.; Ray, S. K.; Dhar, A. Photoinduced Charge Transfer and Photovoltaic Energy Conversion in Self-Assembled *N*, *N*′-Dioctyl-3,4,9,10-perylenedicarboximide Nanoribbons. *Appl. Phys. Lett.* **2010**, *97*, 043306.
31. Li, C.; Liu, M.; Pschirer, N. G.; Baumgarten, M.; Müllen, K. Polyphenylene-Based Materials for Organic Photovoltaics. *Chem. Rev.* **2010**, *110*, 6817–6855.
32. Zhan, X.; Tan, Z.; Domercq, B.; An, Z.; Zhang, X.; Barlow, S.; Li, Y.; Zhu, D.; Kippelen, B.; Marder, S. R. A High-Mobility Electron-Transport Polymer with Broad Absorption and Its Use in Field-Effect Transistors and All-Polymer Solar Cells. *J. Am. Chem. Soc.* **2007**, *129*, 7246–7247.
33. Sicot, L.; Geffroy, B.; Lorin, A.; Raimond, P.; Sentein, C.; Nunzi, J.-M. Photovoltaic Properties of Schottky and p-n Type Solar Cells Based on Polythiophene. *J. Appl. Phys.* **2001**, *90*, 1047–1055.
34. Fabiano, S.; Chen, Z.; Vahedi, S.; Facchetti, A.; Pignataro, B.; Loi, M. A. Role of Photoactive Layer Morphology in High Fill Factor All-Polymer Bulk Heterojunction Solar Cells. *J. Mater. Chem.* **2011**, *21*, 5891–5896.
35. Alam, M. M.; Jenekhe, S. A. Efficient Solar Cells from Layered Nanostructures of Donor and Acceptor Conjugated Polymers. *Chem. Mater.* **2004**, *16*, 4647–4656.
36. Halls, J. J. M.; Walsh, C. A.; Greenham, N. C.; Marseglia, E. A.; Friend, R. H.; Moratti, S. C.; Holmes, A. B. Efficient Photodiodes from Interpenetrating Polymer Networks. *Nature* **1995**, *376*, 498–503.
37. Yu, G.; Heeger, A. J. Charge Separation and Photovoltaic Conversion in Polymer Composites with Internal Donor/Acceptor Hetrojunctions. *J. Appl. Phys.* **1995**, *78*, 4510–4516.
38. Bottari, G.; de la Torre, G.; Guldi, D. M.; Torres, T. Covalent and Noncovalent Phthalocyanine–Carbon Nanostructure Systems: Synthesis, Photoinduced Electron Transfer, and Application to Molecular Photovoltaics. *Chem. Rev.* **2010**, *110*, 6768–6816.
39. Klare, J. E.; Murray, I. P.; Goldberger, J.; Stupp, S. I. Assembling p-Type Molecules on Single Wall Carbon Nanotubes for Photovoltaic Devices. *Chem. Commun.* **2009**, 3705–3707.
40. Ohtani, M.; Kamat, P. V.; Fukuzumi, S. Supramolecular Donor–Acceptor Assemblies Composed of Carbon Nanodiamond and Porphyrin for Photoinduced Electron Transfer and Photocurrent Generation. *J. Mater. Chem.* **2010**, *20*, 582–587.
41. Bindl, D. J.; Safron, N. S.; Arnold, M. S. Dissociating Excitons Photogenerated in Semiconducting Carbon Nanotubes at Polymeric Photovoltaic Heterojunction Interfaces. *ACS Nano* **2010**, *4*, 5657–5664.
42. Tung, V. C.; Chen, L.-M.; Allen, M. J.; Wassei, J. K.; Nelson, K.; Kaner, R. B.; Yang, Y. Low-Temperature Solution Processing of Graphene–Carbon Nanotube Hybrid Materials for High-Performance Transparent Conductors. *Nano Lett.* **2009**, *9*, 1949–1955.
43. Dissanayake, N. M.; Zhong, Z. Unexpected Hole Transfer Leads to High Efficiency Single-Walled Carbon Nanotube Hybrid Photovoltaic. *Nano Lett.* **2011**, *11*, 286–290.
44. Ham, M.-H.; Paulus, G. L. C.; Lee, C. Y.; Song, C.; Kalantarzadeh, K.; Choi, W.; Han, J.-H.; Strano, M. S. Evidence for High-Efficiency Exciton Dissociation at Polymer/Single-Walled Carbon Nanotube Interfaces in Planar Nano-Heterojunction Photovoltaics. *ACS Nano* **2010**, *4*, 6251–6259.
45. Camaioni, N.; Ridolfi, G.; Fattori, V.; Favaretto, L.; Barbarella, G. Branched Thiophene-Based Oligomers as Electron Acceptors for Organic Photovoltaics. *J. Mater. Chem.* **2005**, *15*, 2220–2225.
46. Ooi, Z. E.; Tam, T. L.; Shin, R. Y. C.; Chen, Z. K.; Kietzke, T.; Sellinger, A.; Baumgarten, M.; Mullen, K.; deMello, J. C. Solution Processable Bulk-Heterojunction Solar Cells Using a Small Molecule Acceptor. *J. Mater. Chem.* **2008**, *18*, 4619–4622.
47. Shin, R. Y. C.; Kietzke, T.; Sudhakar, S.; Dodabalapur, A.; Chen, Z.-K.; Sellinger, A. n-Type Conjugated Materials Based on 2-Vinyl-4,5-dicyanoimidazoles and Their Use in Solar Cells. *Chem. Mater.* **2007**, *19*, 1892–1894.
48. Holcombe, T. W.; Norton, J. E.; Rivnay, J.; Woo, C. H.; Goris, L.; Piliego, C.; Griffini, G.; Sellinger, A.; Brédas, J.-L.; Salleo, A.; *et al.* Steric Control of the Donor/Acceptor Interface: Implications in Organic Photovoltaic Charge Generation. *J. Am. Chem. Soc.* **2011**, *133*, 12106–12114.
49. Noone, K. M.; Strein, E.; Anderson, N. C.; Wu, P.-T.; Jenekhe, S. A.; Ginger, D. S. Broadband Absorbing Bulk Heterojunction Photovoltaics Using Low-Bandgap Solution-Processed Quantum Dots. *Nano Lett.* **2010**, *10*, 2635–2639.
50. Palaniappan, K.; Murphy, J. W.; Khanam, N.; Horvath, J.; Alshareef, H.; Quevedo-Lopez, M.; Biewer, M. C.; Park, S. Y.; Kim, M. J.; Gnade, B. E.; *et al.* Poly(3-hexylthiophene)–CdSe Quantum Dot Bulk Heterojunction Solar Cells: Influence of the Functional End-Group of the Polymer. *Macromolecules* **2009**, *42*, 3845–3848.
51. Cheyns, D.; Vasseur, K.; Rolin, C.; Genoe, J.; Poortmans, J.; Heremans, P. Nanoimprinted Semiconducting Polymer Films with 50 nm Features and Their Application to Organic Heterojunction Solar Cells. *Nanotechnology* **2008**, *19*, 424016.
52. Andrew, T. L.; Cox, J. R.; Swager, T. M. Synthesis, Reactivity, and Electronic Properties of 6,6-Dicyanofulvenes. *Org. Lett.* **2010**, *12*, 5302–5305.
53. Mihailetchi, V. D.; van Duren, J. K. J.; Blom, P. W. M.; Hummelen, J. C.; Janssen, R. A. J.; Kroon, J. M.; Rispens, M. T.; Verhees, W. J. H.; Wienk, M. M. Electron Transport in a Methanofullerene. *Adv. Funct. Mater.* **2003**, *13*, 43–46.